The contribution of landsat 8 oli multispectral data to the lithological mapping of the Ait Ourir basin (Western High Atlas, Morocco)

Nidsaid Zaina*, Algouti Ahmed, Algouti Abdellah, Hadach Fatiha and Moujane Said
Cadi Ayyad University, Faculty of Sciences, Department of Geology, Geosciences, Geotourism, Natural Hazards and Remote Sensing Laboratory, Bd. BO 2390, 40000 Marrakech, MOROCCO
*zaina94.nidsaid@gmail.com

Abstract
The present work consists in identifying the geological facies and defining the dominant orientation of the lineaments in order to improve the knowledge on the local geodynamics in the Northern Sub-Atlasic zone of the Marrakesh High Atlas, the Ait Ourir basin region, The latter is characterized by a post-Hercynian Mesozoic cover folded into broad synclines with flat and subhorizontal bottom, separated by ejective and sharp anticlines. For this purpose, multispectral data from Landsat 8 operational land imager (OLI) have been applied in a platform of ArcGIS software and through the treatments offered by this software, namely, the principal component analysis (PCA), the band ratios (BR) and the transformation of the minimum noise fraction (MNF), a better lithological discrimination and description was brought to the set of geological formations that form the studied basins.

In parallel, the results obtained by the method of classification by Support Vector Machine (SVM), which is based on the joint use of geomorphic features, textures and multispectral data from Landsat 8 satellite, showed an excellent correlation. With the simplified geological map of the northern slope of the High Atlas of Marrakesh (1/10000) and field data from the study area. The result shows an overall accuracy of classification of Landsat8 OLI data by SVM which is 96.64% and the Kappa coefficient which is 0.98 and a positive correlation is shown between lineament structures and dominant orientations of the extracted lineaments. The highest densities obtained are N-S, NE-SW and NNE-SSW oriented with the predominance of the first direction.

Keywords: Lithologic mapping, Landsat OLI, Lineaments, SVM, PCA, Morocco.

Introduction

Geological mapping consists in identifying the different rock types in a given area while describing their features (composition, stratigraphy and structures) and then proceeding to map the geological data collected in the field. The detection of linear structures can be done either by visual extraction or by automatic extraction by the Geomatica software. A lineament is a simple or compound linear feature, detected on the surface whose different parts are aligned along a line or a curve[20].These lineaments result from structural deformations in the Earth's crust under different geomorphological aspects (faults, folds and fractures)[8,20,23].

In this context, the use of remote sensing is a valuable tool to complement the data already obtained. Indeed, spatial remote sensing, especially in arid environments, helps to identify formations, to highlight most of the major geological structures (lineaments, lithological contacts) and to obtain valuable structural indications (trajectories of schistosity or foliation) by multiplying the observation and exploration capabilities of the geologist[14].

The objective of this study is to enhance the contrast and detail of our Landsat 8 OLI image by applying various image processing and enhancement methods such as principal component analysis, ratios, MNF, SVM and directional filters. These processing methods enhanced the original images and thus facilitated the visualization and detection of lineaments.

Geographical, geological and stratigraphic setting of the Ait Ourir basin

The study area is located on the northern sub-Atlasic zone of the Marrakesh Hight Atlas[18]. It is bound on the north by the Haouz plain, the south by the highlands, west by Oued Ourika and east by Oued R'dat (Fig. 1).

The Ait Ourir basin is covered by a post-Hercynian Mesozoic cover folded into broad synclines with flat and subhorizontal bottoms, separated by ejective and acute anticlines[13,21]. These anticlinal structures are associated with regional faults related to an active halokinetic activity proved by the installation of local angular discordance and variation in thickness and facies[13].

For example, in the Jbel Sour basin, the western sector is formed by detrital coarse sediments deposited in the context of a fluvial dynamic whereas the eastern sector is characterized by an essentially carbonate-evaporitic sedimentation, in a shallow and confined environment, subjected to an important subsidence, under a hot and arid climate favoring the formation of sebkha facies. Synthetic stratigraphic log shows significant diversity (Fig. 1c).

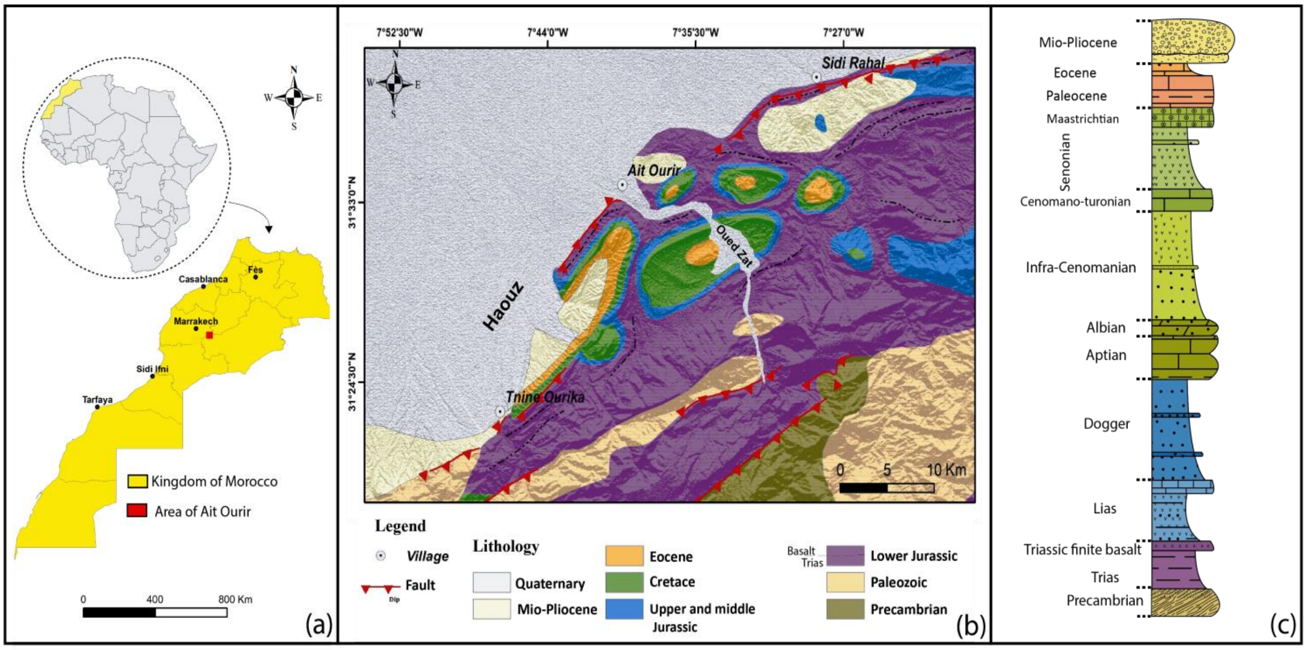

By Z. NIDSAID / 2GRNT - 2021/ Cadi Ayyad University.

Figure 1: (a) Geographical location of sector on map of Morocco, (b) Simplified geological map (Ait Ourir 1 /10,000), (c) Lithostratigraphic column of the study area.

Table 1
Simplified stratigraphic overview of the study area

Age	Lithology (including bibliographic references)
Paleozoic	Shales and grey sandstones
Triassic	Three types of units are distinguished, one dominated by sandstone-conglomerates, the other by the clay-salt (F6) which ends with the finite-triassic Basalts[16]
Lias	alternating clays and red silt with gypsum overlaid by dolomitic limestone
Dogger	Terrigenous red detrital deposits represented by alternating conglomerate and sandstone, silt and clay
Aptian-Albian	Sedimentary succession is composed by calcareous and dolomitic marls with rudist and dolomitic limestones with corals, it ends with sandy-limestones[13]
Infra-Cenomanian	Consists by red silty-sandstone with intercalated conglomeratic deposits
Cenomanian-Turonian	Essentially made up of a dolomitic limestone formation, often massive at the base and laminated at the top with a transgressive tendency[18]
Senonian	Marl and red sandstone with gypsum characteristic of a coastal sebkha at Jbel Sour[4,5,7]
Maastrichtian-Eocene	Marls with evaporites, phosphate limestones and flint limestones[18]
Mio-Pliocene	Sandstone and conglomeratic deposits, products of Atlas chain weathering
Quaternary	It is presented either in the alluvial cones, or in the deposit of major river beds

Material and Methods

Data: The dataset used for this study is from EE (EarthExplorer) the online search, discovery and ordering tool developed by the United States Geological Survey (USGS). Landsat 8 OLI data are taken by the Operational Land Imager (OLI) sensor and referenced LC08_L1TP_202038_20191216_20191226_01_T1 and correspond to the Path202/Row38 scene taken on 12 December 2019. This scene has the characteristics presented in table 2 with a Universal Transverse Mercator (UTM) zone 29 projection of the World Geodetic System North WGS 84 datum.

Pre-treatments and treatments: Pre-processing operations are essential to obtain spatially and radiometrically corrected images to analyze and compare spectral data.

Instrumental crosstalk effects and the atmospheric effect are abnormally of high radiance in bands 5 and 9 due to the transmission of energy from band 4 optical elements to adjacent detectors in bands 5 and 9.

Therefore, the corrected crosstalk of the L8 OLI image is calibrated to the surface reflectance using the Fast Line of Sight Atmospheric Analysis Spectral Hypercubes (FLAASH) model which incorporates the Moderate Resolution Transmittance (MODTRAN) radiation transfer code to remove atmospheric attenuation in order to produce a reflectance image. The methodological approach adopted is summarized in fig. 2.

Table 2
Salient characteristics of Landsat-8 Operational Land Imager (OLI)

Bands	Wavelenghts (µm)	Resolution (m)
Band 1 - Coastal aerosols	0,433 – 0,453 µm	30m
Band 2 - Blue	0,450 – 0,515 µm	30m
Band 3 - Green	0,525 – 0,600 µm	30m
Band 4 - Red	0,630 – 0,680 µm	30m
Band 5 - NIR	0,845 – 0,885 µm	30m
Band 6 – SWIR 1	1,560 – 1,660 µm	30m
Band 7 – SWIR 2	2,100 – 2,300 µm	30m
Band 8 - Panchromatic	0,500 – 0,680 µm	15m
Band 9 - Cirrus	1,360 – 1,390 µm	30m

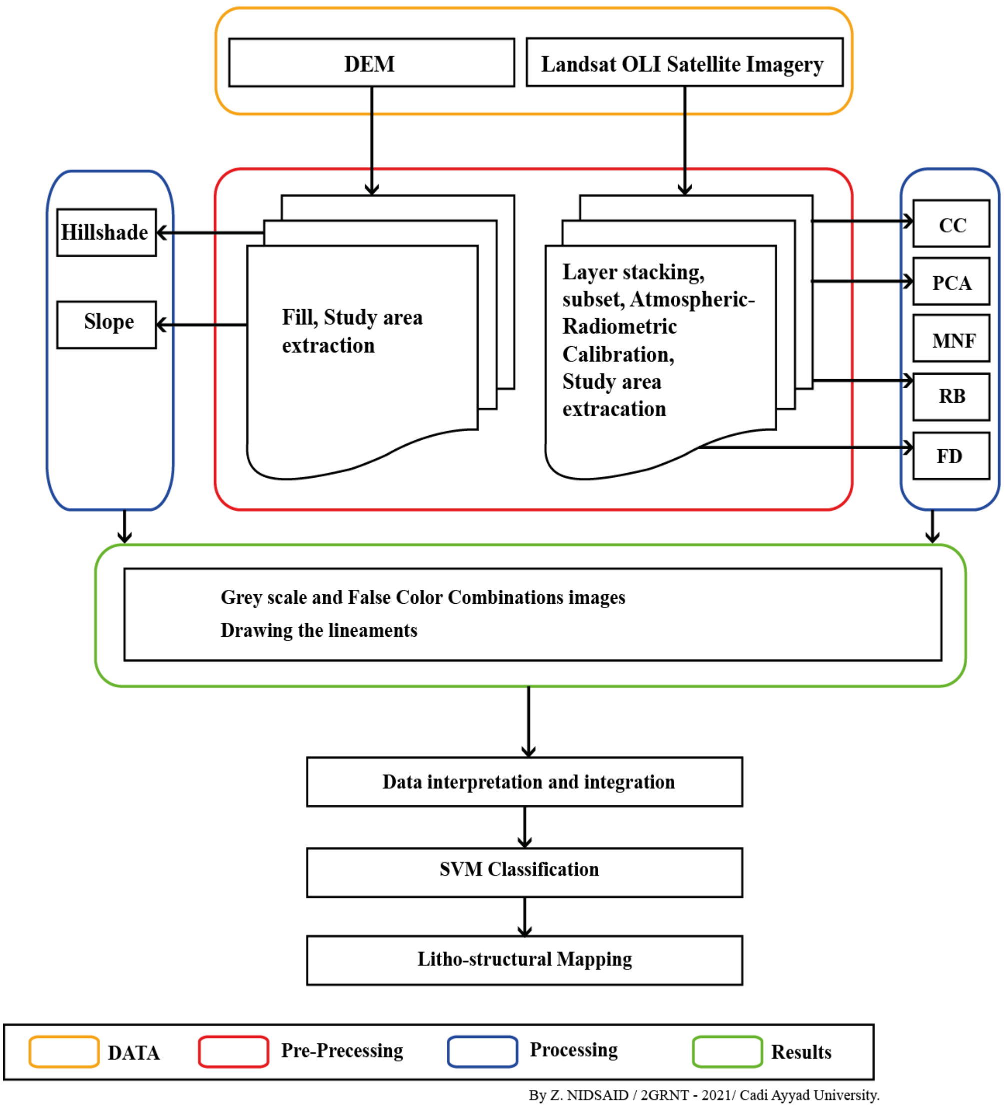

Figure 2: Methodology flowchart of the present study

Results and Discussion

Band ratio: Band ratio images improve the contrast between features by dividing the brightness values at peaks and troughs in a reflectance curve after removing atmospheric conditions from the image. Spectral band rationing improves compositional information while removing other types of information about the Earth's surface. This method is used for highlighting certain features or materials that are not visible in the raw bands[22]. For the calculation of band ratios, we took the least correlatable that allowed us to make new compositions colored. In the case of our study area, the compositions that have provided the best results are: (4/3, 6/7, 5/6 as RGB) and (6/4; 4/2; 5/4 as RGB) (Fig. 3).

The ratio 4/2 were executed for mapping ferric iron oxides because of their absorption capability in the blue spectral region and high reflectance in the red spectral region[10]. The ratio 6/7 was used in this study to map kaolinite, montmorillonite and clay minerals. These features have a high reflectance on band 6 and low reflectance in band 7 of Landsat 8 image. The ratio 6/5 is useful for mapping iron minerals due to the high reflectance of these minerals in this ratio[12].

Minimum Noise Fraction Transform (MNF) : The MNF analysis can identify the locations of spectral signature anomalies. This process is important to exploration geologists because spectral anomalies are often indicative of alteration due to lithologic units and hydrothermal mineralization.

The application of the MNF technique on the OLI subset data gives us 7 MNF images of OLI. A plot of Eigen values versus MNF band number shows a sharp decrease in the magnitude between 1 and 7 for OLI.

In this study, MNF components with values not exceeding 1 are generally excluded from the data as noise in order to improve the results of further spectral processing[19]. MNF components of 1, 2 and 3 are assigned to the RGB band combination of Landsat OLI data presented here. In the study area, the results show that the basaltic rock units are detected by a light blue hue, the dolomitic limestone appears by a navy-blue hue and the vegetated region is green in color (Fig. 4).

Principle component analysis (PCA): In this study, we applied this technique widely used within the remote sensing, to the different spectral domains in order to condense the information distributed in the many spectral bands of our Landsat OLI scene[6]. The new components typically represent up to 97% of the original or initial data set[9]. PCA components 7, 2 and 6 are assigned to the RGB band combination of Landsat 8 OLI data (Fig. 5).

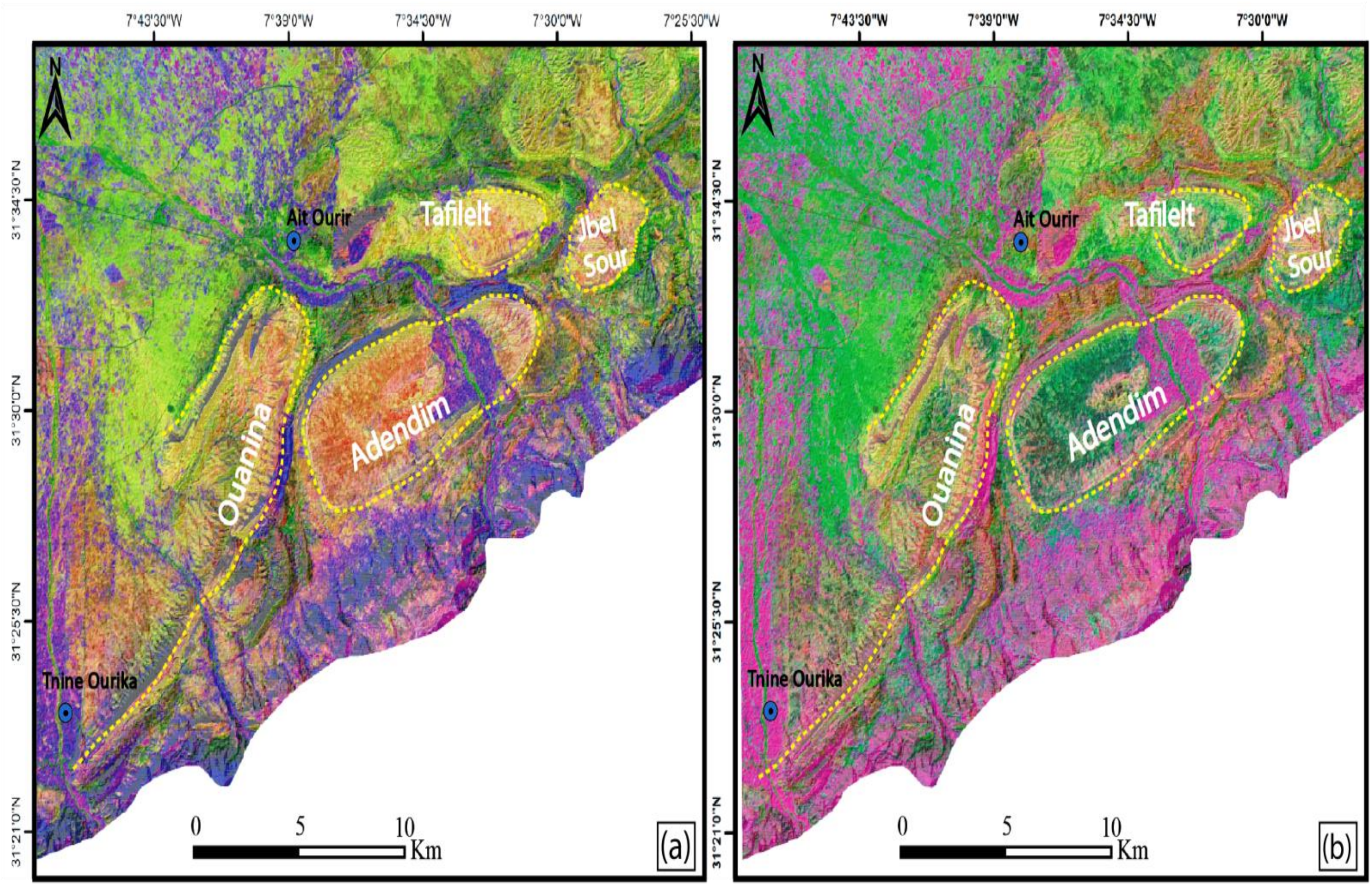

Figure 3: Landsat8 OLI band ration color image, (a) (4/3, 6/7 and 5/6 as RGB), (b) (6/4, 4/2 and 5/4 as RGB).

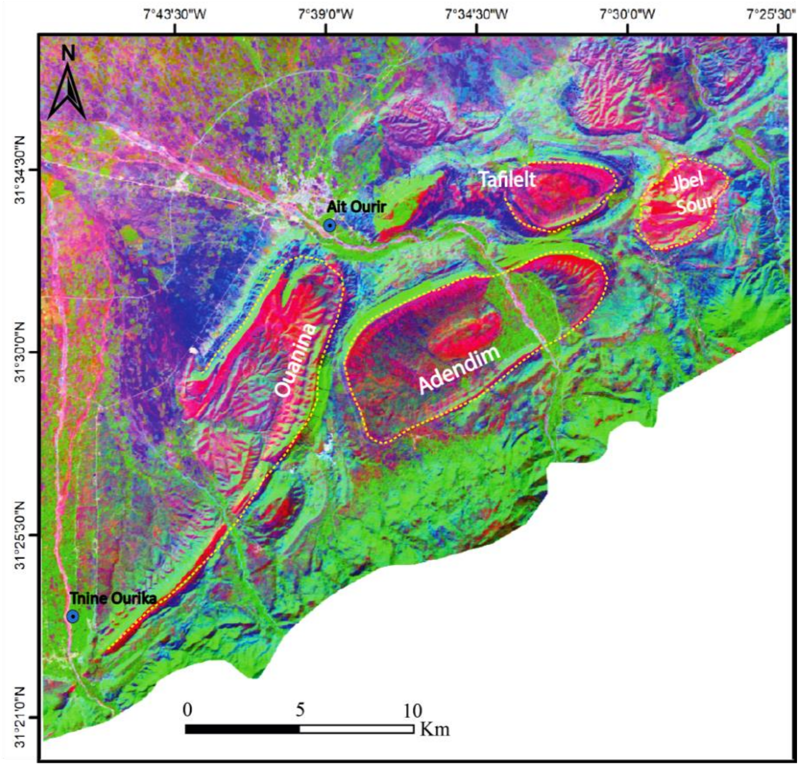

Figure 4: MNF1, MNF2 and MNF3 of OLI image

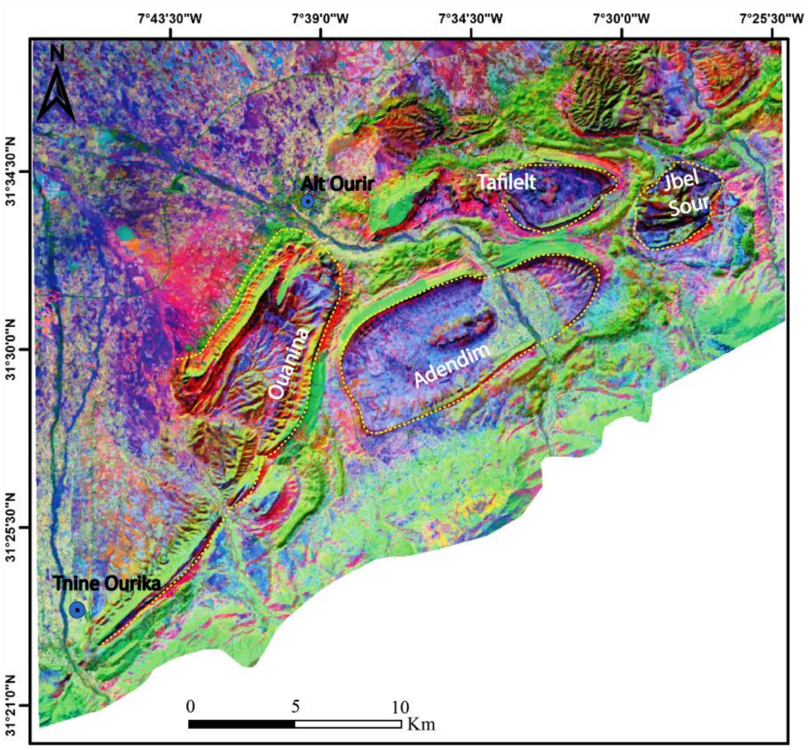

Figure 3: Color Composite (PC1, PC2 and PC3 as RGB).

In the totality of the image, we can recognize the basaltic series in light green. The quaternary is presented in light pink and the red silt with gypsum by dark pink colors.

SVM Classification: For optimized lithological classification of the study area from remote sensing data, we experimented by training SVMs using various combinations of input data selected from Landsat OLI images. ROIs covering different lithological units using geological map, field data and Google Earth aerial images.

Towards the end of the classification, the accuracy was evaluated by calculating the confusion matrix by comparing pixel by pixel the classification result and the field data.

Examination of the confusion matrix shows an overall accuracy of 96.64% with a kappa coefficient that is 0.98. The diagnostic of the diagonals of confusion matrixes shows that the OLI sensor gave better results, sandstone-clay and triassic finite basalt of Trias, the red bed of Dogger and infra, Limestone dolostone of CT and Limestone of Eocene.

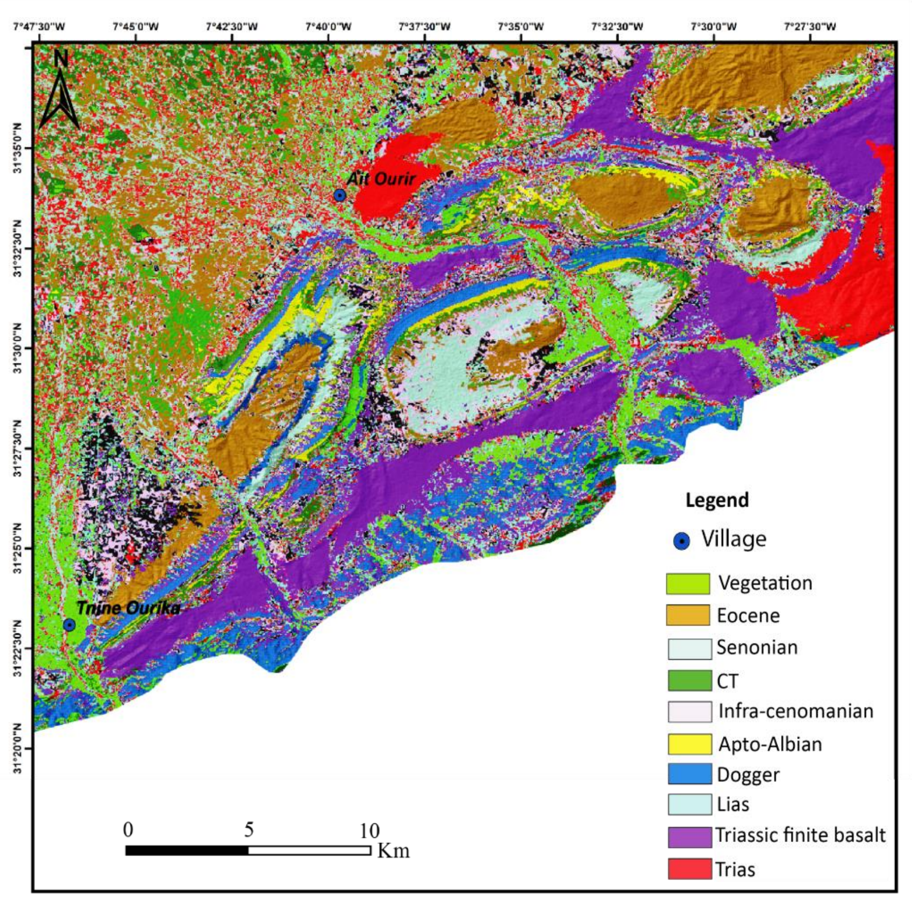

Figure 4: SVM classification results.

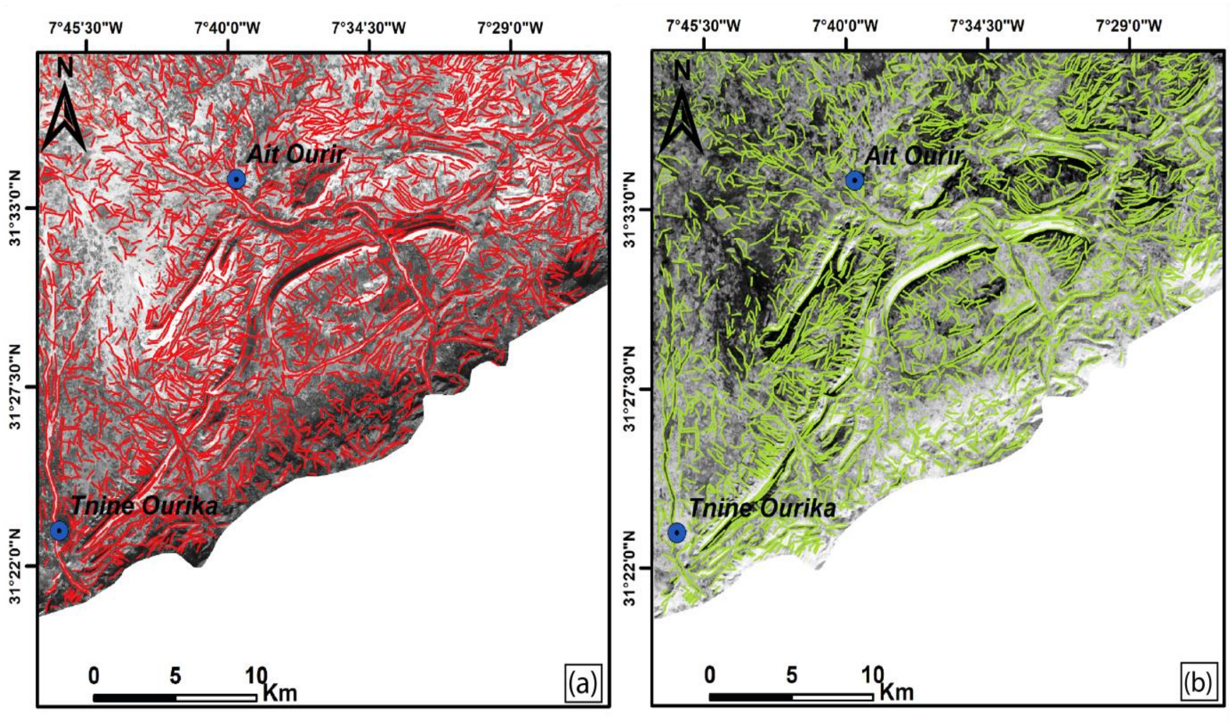

Figure 5: Total Lineaments maps extracted, (a) from band 8 (b) from the PC1 image

Directional Filters: Directional filters are widely used in geology to detect lineaments. When applying the Sobel 45° and 90° directional filters, we chose the 5*5 matrix which generated images with sufficient detail for lineament detection[15] on the principal components from PC1 and band 8 (Fig. 7). This allows us to enhance the contours and extract the directions of geological discontinuities in the image[17].

In this study, two methods of extraction lineaments from satellite images were used, the automated extraction is performed by the LINE module of Geomatica software and the visual lineament extraction in which the lineaments are drawn manually based on a visual interpretation (Fig. 8). The overlay with the topographic map allows to remove by geoprocessing all the anthropic linear structures identified on the image (roads and trails) (Fig. 9a and b).

Manual lineament detection is performed on the transformed strips. The superposition of the information contained in the images used for the manual tracing made it possible to create the lineament map. The directions chosen for the lineament maps were a= 45° and a =90°. The population of lineaments and the maximum concentrations are at N-S, NE-SW, NW-SE and NNW-SSE directions (Fig.10).

The morphological aspect of the Ait Ourir region is underlined by rather marked structural reliefs curved in ellipse arcs in the form of elongated ridges and directions NE-SW to E-W, this landscape gives the region its originality by drawing basins with altitude varying between 900 and 1100 metres corresponding to perched synclines separated by eroded anticlines where the wadis have cut their beds. The present study focuses on the processing and interpretation of a Landsat 8 OLI multispectral and panchromatic scene of a panchromatic band 8 OLI with a spatial resolution of 15 m of the Ait Ourir area.

However, for a good Lithological and Structural lineament Mapping, we have adopted some techniques namely the calculate band ratios by taking the least correlatable. The ratio 4/2 is useful for mapping iron oxides because it has absorption in the blue region, where it has high reflectance in the red region[10].

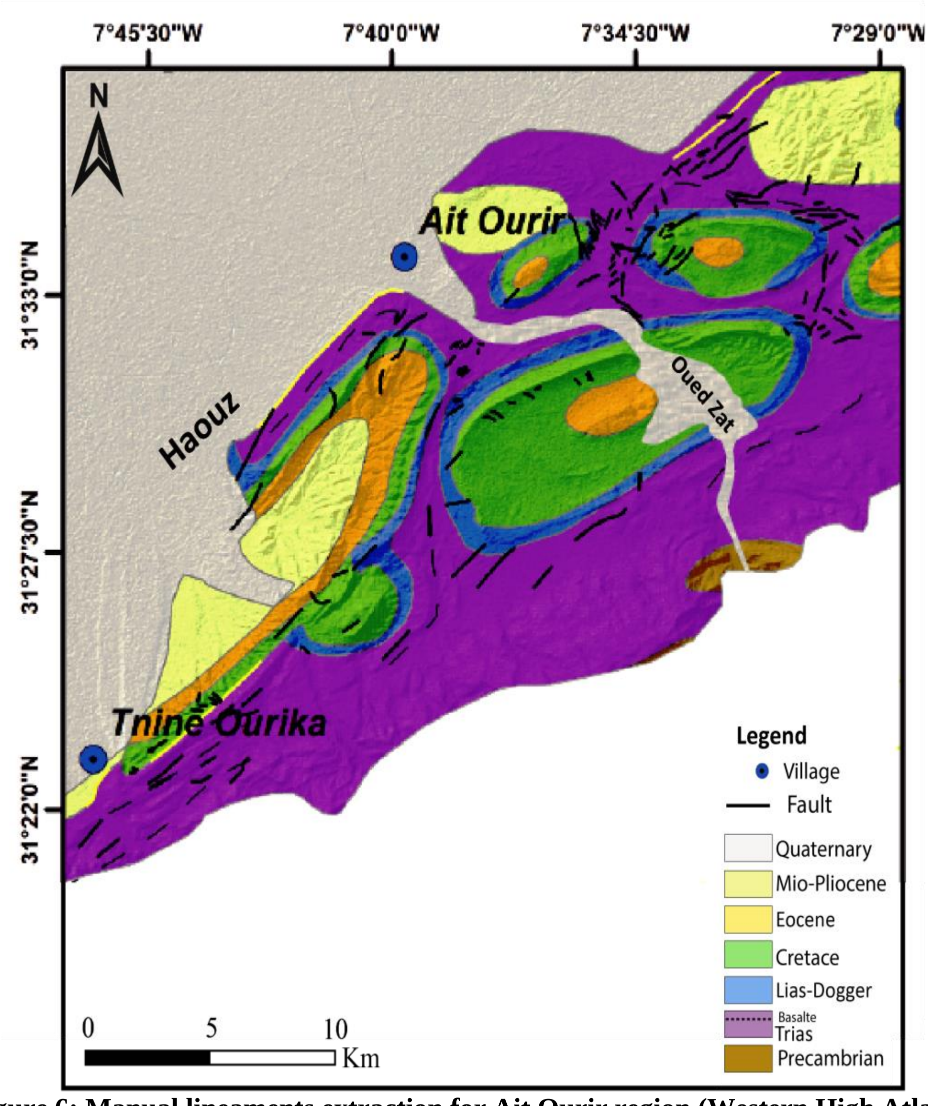

Figure 6: Manual lineaments extraction for Ait Ourir region (Western High Atlas).

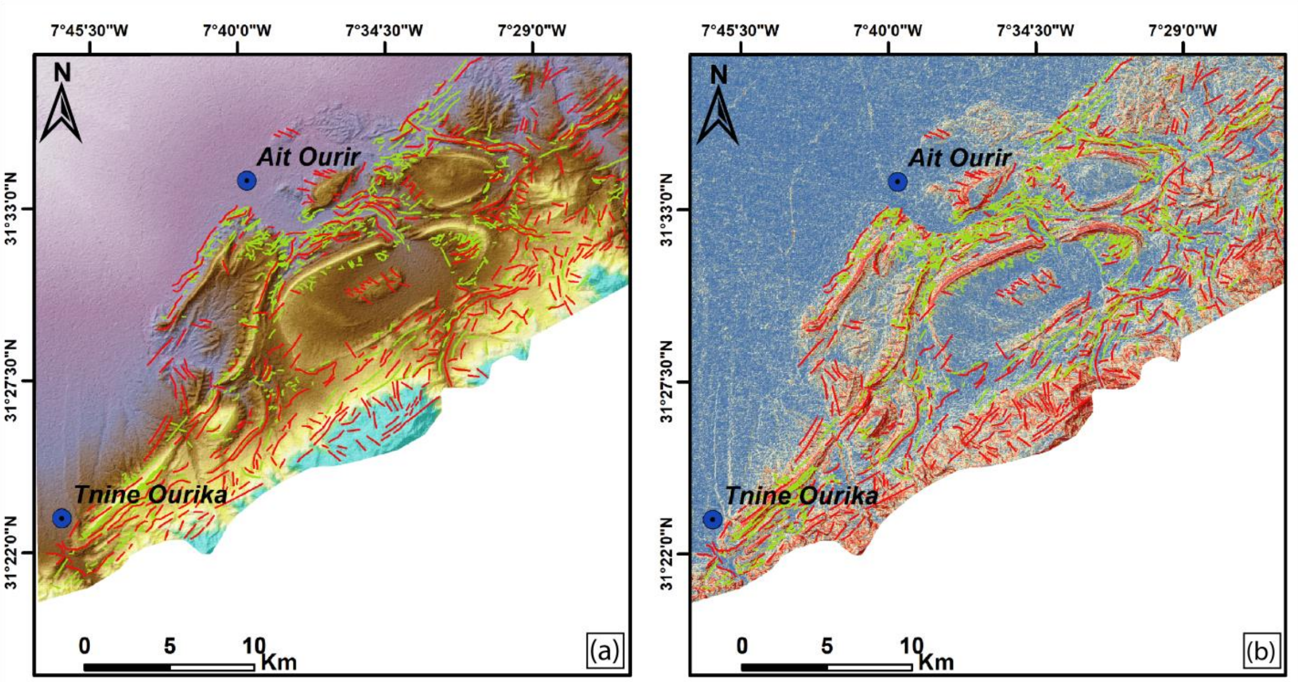

Figure 7: Total lineaments from the directional filters: (a) PC1-B8 lineament/DEM correction (b) PC1-B8 /slope correction (red line represents B8 lineaments, green represents PC1 lineaments)

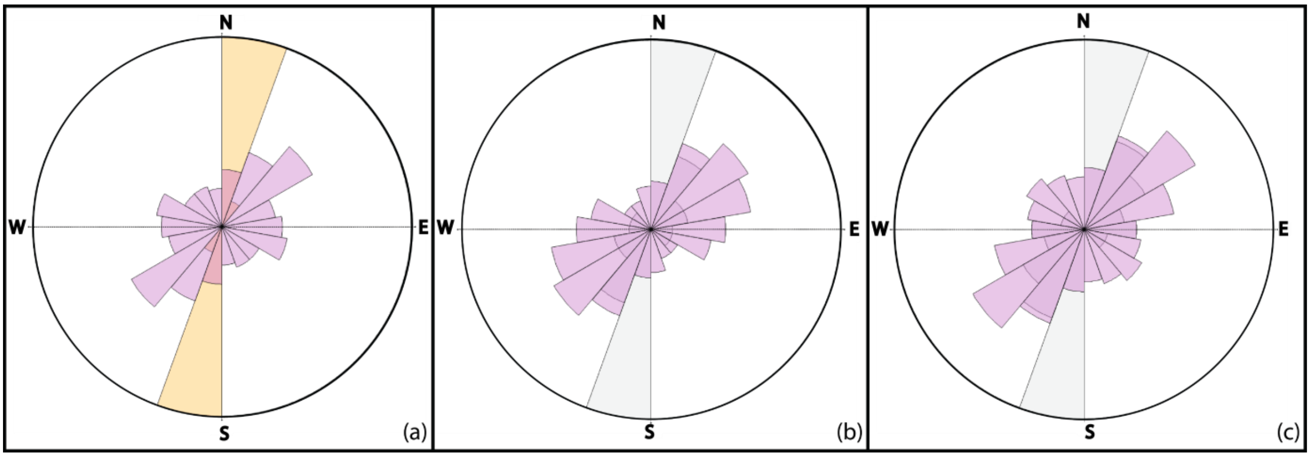

Figure 8: Orientations of lineaments obtained from the (a) band 8 (automatic lineament extraction), (b) from PC1 (automatic lineament extraction) and (c) Manual lineaments extraction

The ratio 6/7 was used in this study for its ability to map kaolinite, montmorillonite and other clay minerals. In the study area, the percentage of kaolinite is relatively low and is associated with levels of siltstone and clay. Therefore, the origin of this kaolinite is probably detrital and would reflect relatively declining landforms in warm climates and relatively hydrolyzing.

We note the presence of illite with very important percentages, their abundance suggests an active erosion of the backcountry. It probably derived from the surface alteration of pre-existing phyllite minerals. The ratio 6/5 was applied to map ferrous minerals due to the high reflectance of these minerals in this ratio[12]. Some authors have applied this band-ratio technique in their studies namely additional bands (7+9)/8 and (5+7)/6 allowed the identification of two main sets of hydrothermal alteration minerals which are sericite, smectite, illite and muscovite on the one hand and chlorite, epidote, carbonates on the other, in the central jebilets region, Morocco[2].

Although the MNF components showed that the basaltic rock units are detected as light blue hue, the dolomitic limestones appearing as dark blue color and the vegetated region as green color in the study area, while the results of the principal component analysis (PCA) showed that the quaternary is represented by light pink pixels, red silt with gypsum in dark pink and basalts in light green. Both techniques are widely used by several authors in the Central High Atlas to describe geological formations. Statistical analysis and observation of the lineament map also revealed two major families of orientation, major structures-oriented

N-S and minor structures-oriented NNE-SSW. The N-S direction, the most important in the sector, represents the main orientation of the High Atlasic fault (NE-SW). Minor lineaments have been identified and recognized in the field as faults.

The comparison of fracture orientation shows a good correlation with previous work in the Eastern Anti-Atlas[3] well approved the direction of lineaments by Landsat-8, ASTER and Sentinel 1 satellite at the inlier of Sidi Flah-Bouskour, Moroccan Anti-Atlas. The direction of lineament is generally NE-SW and E-W. Similarly, the general direction of the lineaments in the Kammouna Arid Area (Eastern Anti-Atlas, Morocco)[11] showed three directions (E-W, N-S, NE-SW) which are almost the same as those mentioned in our study area. In comparison, lineaments orientations have shown a good correlation with earlier work on automatic lineaments extraction in the Ikniouen area, Eastern Anti-Atlas, Morocco[1].

Conclusion

We examined the usefulness of Landsat 8 OLI data for lithologic mapping in the zone of the Ait Ourir Basin, the high Atlas Mountains of Marrakech. According to this study, lithological units such as sandstone-clay and basalt of the Triassic, the Red Beds of Dogger and Infra, CT dolomitic limestone and Eocene limestone are well mapped in the OLI image using SVM classification whose overall accuracy is 97.28% and Kappa coefficient is 0.97.

Statistical analysis and observation of the lineament map also revealed two major orientation families, major structures-oriented N-S and minor structures-oriented NNE-SSW that could be easily observed in the field. So, it is a powerful tool to get a quick overview of the structure of this area.

The use of remote sensing requires a lot of precaution while saving time in terms of geological and structural mapping while mapping by conventional methods (tracking faults in the field, aerial photographs) requires a lot of time and does not always identify all existing lineaments, but it remains the more reliable of the two methods in terms of characterization of the lineaments detected.

Acknowledgement

The authors would like to thank the NAZA-USGS GLOVIS-GATE for the OLI data. We also thank you to our teachers for their support and encouragements.

References

1. Abdelouhed F., Ahmed A., Abdellah A. and Mohammed I., Lineament mapping in the ikniouen area (Eastern Anti-Atlas, Morocco) using Landsat-8 Oli and SRTM data, *Remote Sensing Applications: Society and Environment*, **23**, 100606 **(2021a)**

2. Abdelouhed F., Algouti Ahmed, Algouti Abdellah, Mohammed I. and Mourabit Z., Contribution of gis and remote sensing in geological mapping, lineament extractions and hydrothermal alteration minerals mapping using aster satellite images: case study of central jebilets-morocco, *Disaster Advances*, **14(1)**, 15–25 **(2021)**

3. Adiri Z., El Harti A., Jellouli A., Lhissou R., Maacha L., Azmi M., Zouhair M. and Bachaoui E.M., Comparison of Landsat-8, ASTER and Sentinel 1 satellite remote sensing data in automatic lineaments extraction: A case study of Sidi Flah-Bouskour inlier, Moroccan Anti Atlas, *Advances in Space Research*, **60**, 2355–2367 **(2017)**

4. Algouti A., Turonien supérieur et Sénonien du versant nord du Haut-Atlas de Marrakech, Caractérisation sédimentologique et strati-graphique **(1991)**

5. Algouti Ah, Algouti Ab and Taj-Eddine K., Le Sénonien du Haut Atlas occidental, Maroc: sédimentologie, analyse séquentielle et paléogéographie, *Journal of African Earth Sciences*, **29**, 643–658, https://doi.org/10.1016/S0899-5362(99)00121-9 **(1999)**

6. Antoine D., Travaux Pratiques de télédétection spatiale, Arlon Campus Environnement, Université de Liège, Belgique, 84 **(2013)**

7. Azzaoui K.A. and Azzaoui K.A., Etude lithostratigraphique. Sédimentologique et cartographique du Sénonien du jbel Sour (Haut Atlas de Marrakech), Mém. C.E.A. Univ. Caddi Ayyad, Marrakech? Maroc. **(1983)**

8. Clark C.D. and Wilson C., Spatial analysis of lineaments, *Computers & Geosciences*, **20**, 1237–1258 **(1994)**

9. Deslandes S., Initiation aux méthodes de traitement numérique des images satellites, sur le système PCI Inc., EASUPACE CARTEL, 32 **(1989)**

10. El Atillah A., Zine E.M.Z. and Souhassou M., Utilisation de l'image multi spectrale pour l'exploration et la recherche des ressources minérales: état des connaissances et proposition d'un modèle de traitement, *European Scientific Journal*, **14(24)**, 350 **(2018)**

11. Es-Sabbar B., Essalhi M., Essalhi A. and Mhamdi H.S., Lithological and structural lineament mapping from Landsat 8 OLI images in Ras Kammouna arid area (Eastern Anti-Atlas, Morocco), *Economic and Environmental Geology*, **53**, 425–440 **(2020)**

12. Gupta R.P., Remote sensing geology, Springer **(2017)**

13. Hadach F., Aptian–Albian deposits of the Ait Ourir basin (High Atlas, Morocco): New additional data on their paleoenvironment, sedimentology and palaeogeography, *Open Geosciences*, **12**, 1557–1572 **(2020)**

14. Hammad N., Apport de la télédétection à haute résolution à la discrimination lithologique en domaine semi désertique et aride, application à la région du Djebel Drissa (massif des Eglab), Ph.D. Thesis **(2008)**

15. Hornsby J. and Bruce B., A preliminary analysis of Landsat MSS and TM data in the Levack area, sudbury, Canada, In 1985 International Geoscience and Remote Sensing Symposium (IGARSS'85), Amherst, MA, 131–140 **(1985)**

16. Michard A., Eléments de Géologie Marocaine **(1976)**

17. Moore G.K. and Waltz F.A., Objective procedures for lineament enhancement and extraction, *Photogrammetric Engineering and Remote Sensing*, **49**, 641–647 **(1983)**

18. Moret L., Recherches géologiques dans l'Atlas de Marrakech, Protectorat de la République française au Maroc Direction générale des **(1931)**

19. Morris J.T., Porter D., Neet M., Noble P.A., Schmidt L., Lapine L.A. and Jensen J.R., Integrating LIDAR elevation data, multi-spectral imagery and neural network modelling for marsh characterization, *International Journal of Remote Sensing*, **26**, 5221–5234 **(2005)**

20. O'leary D.W., Friedman J.D. and Pohn H.A., Lineament, linear, lineation: some proposed new standards for old terms, *Geological Society of America Bulletin*, **87**, 1463–1469 **(1976)**

21. Rey J., Canérot J., Peybernès B., Taj-Eddine K. and Thieuloy J.P., Lithostratigraphy, biostratigraphy and sedimentary dynamics of the Lower Cretaceous deposits on the northern side of the western High Atlas (Morocco), *Cretaceous Research*, **9**, 141–158 **(1988)**

22. Rockwell B.W. and Hofstra A.H., Identification of quartz and carbonate minerals across northern Nevada using ASTER thermal infrared emissivity data—Implications for geologic mapping and mineral resource investigations in well-studied and frontier areas, *Geosphere*, **4**, 218–246 **(2008)**

23. Vassilas N., Perantonis S., Charou E., Tsenoglou T., Stefouli M. and Varoufakis S., Delineation of lineaments from satellite data based on efficient neural network and pattern recognition techniques, Proc. Second Hellenic Conference on AI Citeseer, 355–365 **(2002)**.

(Received 02nd March 2022, accepted 25th April 2022)